Towards the Development of Advanced Packing Design for Distillation in Rotating Packed Beds

Hina Qammar[1], Konrad Gładyszewski[1,2], Andrzej Górak[1,2], and Mirko Skiborowski[1,*]

DOI: 10.1002/cite.201900053

Dedicated to Prof. Dr. techn. Hans-Jörg Bart on the occasion of his 65th birthday

The growing demand for flexible and compact separation technologies has promoted the application of high-gravity technology, like rotating packed beds (RPBs). Mass transfer characterization and packing design play an important role in the development of this technology. This article provides a systematic approach towards the evaluation of packing and the development of advanced packing design for distillation in RPBs. For the latter, an additive manufacturing approach is used to develop a new Zickzack packing for RPBs. The new packing provides better mass transfer at reduced pressure drop compared to available conventional packings, while being competitive in terms of mass transfer with the industrially applied rotating zigzag bed at significantly reduced pressure drop.

Keywords: Distillation, Mass transfer and pressure drop, Packing design, Rotating packed bed, 3D printing

Received: March 01, 2019; *revised:* August 06, 2019; *accepted:* August 14, 2019

1 Introduction

Fluctuations in customer demand bring new challenges to the chemical industry, requiring energy-efficient, cost-effective and modular processes. While distillation is still the most widely used fluid separation technology, it remains a space-demanding and energy-intensive separation process in the chemical industry [1]. Traditionally, multistage countercurrent distillation is implemented in static columns with different types of trays or packed beds. The liquid flow is directed downwards due to the gravitational force, while a vapor flows upwards. A promising concept for intensified distillation equipment is the so-called high gravity (HIGEE) technology and rotating packed beds (RPBs) in specific, which have gained considerable attention in recent years, especially in Asia [2, 3]. They bear the potential for significant mass transfer improvements and extended operating window, compared to static equipment, providing compact equipment with added flexibility. In RPBs, the centrifugal force induced by rotation of a packed bed is exploited to intensify the contacting of a gas and a liquid stream, which is passing countercurrently through the packing. This annular-shaped packing is fixed inside a rotor that is mounted to a shaft and surrounded by a casing, as shown in Fig. 2. The liquid is introduced at the inner edge of the annular packing and is accelerated radially outward towards the stationary casing through an applied centrifugal field, while the vapor stream is introduced into the casing and flows radially inward due to an imposed pressure gradient. It is claimed that the application of high shear forces creates thin films and fine droplets, thus leading to intensified contact between the phases [4–6]. Intense mixing, reduced equipment size, use of high specific surface area packings and an enlarged operating window are the main benefits of this technology compared to the conventional gravity-based separation [7].

The concept of centrifugal process intensification has been introduced for the first time more than 80 years ago with a patent by Podbielniak [8]. However, the design of today's RPBs rather relates to the patents by Pilo and Dahlbeck [9], as well as Ramshaw and Mallinson [10]. Especially the work of Ramshaw at ICI on RPBs was of significant importance for promoting the concept of process intensification to the chemical engineering community [6]. Owing to the increasing interest in RPBs, a number of rotor types and packing designs have been developed specifically in the last two decades. The article by Cortes-Garcia et al. [3] provides

[1]Hina Qammar, Konrad Gladyszewski,
Prof. Dr.-Ing. Andrzej Górak, Dr.-Ing. Mirko Skiborowski
mirko.skiborowski@tu-dortmund.de
TU Dortmund University, Department of Biochemical and Chemical Engineering, Laboratory of Fluid Separations, Emil-Figge-Straße 70, 44227 Dortmund, Germany.

[2]Konrad Gladyszewski, Prof. Dr.-Ing. Andrzej Górak
Lodz University of Technology, Faculty of Process and Environmental Engineering, Department of Environmental Engineering, Wólczańska 213, 90-924 Łódź, Poland.

a concise overview and analysis of the available designs with respect to distillation. Experimental investigations have been expanded from conventional single-block packings for RPBs, like wire mesh [11, 12], knit mesh [12] and metal foams [13], to more complex packing and rotor configurations, as in split packing [14] for enhanced vapor angular slip velocity and several other alternatives [15–17].

For continuous distillation applications especially the so-called rotating zigzag beds (RZBs), mainly developed by Wang et al. [18, 19], have shown superior performance compared to known single-block packings in RPB and have resulted in a number of industrial applications, primarily in Asia [3, 20]. Unlike classical RPBs with so-called single-block packings [4], which are fixed in between two simultaneously rotating disks, the RZB rotor consists of a rotating disk and a stationary disk, on which two series of circular baffles are mounted in an alternating fashion. The RZB concept is thereby linked more closely to the concept of tray columns, whereas the conventional RPBs are closely related to packed columns. Although many attempts have been made to exploit the full potential of HIGEE technology, which was initially promoted to enable an equipment size reduction by a factor of 10–100 [21], the industrial application of RPBs, especially in Europe and the US, is still very limited [7]. Potential reasons can be found in a general caution related to rotating equipment, the related energy consumption as well as the lack of dedicated analysis of mass transfer inside the RPB and proper scale-up rules. The existing reservation regarding the mechanical design and maintenance may, however, be unnecessary since RPBs are very similar to centrifugal pumps or centrifuges [22], which are considered as reliable and established technology. However, there is still a severe need for reliable mass transfer analysis and modeling since most published data for RPBs reflect results of rather small-scale laboratory equipment while assuming that all mass transfer in the RPB can be attributed to the packing. As illustrated in a previous work [23] a differentiation between mass transfer in the packing and the casing is, however, of significant importance when characterizing the performance of a specific type of packing for different operating parameters, like rotational speed and *F*-factor. Therefore, different rotor configurations, with and without packing, have to be evaluated, in order to quantify the mass transfer inside the packing and compare the performance of different packings.

In the current study, the experimental investigations of different packings are extended, including a newly developed single-block packing, for which a prototype was produced by means of an additive manufacturing approach through 3D printing [24]. The newly developed Zickzack packing is introduced and compared with conventional knit mesh and metal foam packings based on dedicated batch distillation experiments under total reflux for the dehydration of ethanol. While the Zickzack packing design is oriented towards the geometry of an RZB, it allows for implementation in a classical RPB rotor.

1.1 Development of Zickzack Packing Design

Since an ideal packing should provide the required separation efficiency at minimum possible pressure drop, a trade-off between those targets needs to be found. Such a trade-off can be realized through a combination of the RZB structure and a single-block packing. The major idea for the newly developed single-block packing, called Zickzack (ZZ) packing, is to provide higher residence time compared to RPB packings, such as foams and wire meshes while reducing pressure drop and power consumption compared to RZB.

The initial design of the ZZ packing is illustrated in the form of a cross-section view in Fig. 1. Similar to the RZB, the ZZ packing enforces a zigzag path of the gas and the liquid through the rotor, which results in higher residence time and hold up for gas-liquid contacting. However, unlike in the RZB, in which the upper baffles are fixed to the static disc while the lower baffles are mounted to the rotating disc, the whole ZZ packing is rotating at the same angular speed. Furthermore, the baffles of each stage have no holes (perforation in the vertical wall as described by Wang et al. [18]), such that the liquid is transferred between the stages by overflow.

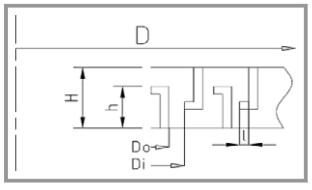

Figure 1. Zickzack packing cross-section sketch.

To maintain a minimum holdup on the different stages a horizontal protrusion on the top of each stage is introduced as an additional feature. The total holdup can be calculated as the sum of the minimal holdup and the volume added by a liquid curvature, depending on the rotational speed. However, as described by Lubarda [25], the curvature will flatten to a point where it can be neglected under the condition that the rotation-induced Bond number is

$$Bo_\omega = \frac{\rho_l D^3 \omega^2}{8\sigma_{lv}} > 20 \tag{1}$$

$$\frac{\left(Do_{i+1}^2 - Di_i^2\right)\pi}{4} = \text{const.} \tag{2}$$

For current packing design, condition $Bo_\omega > 20$ is fulfilled at every stage of the packing when the rotational speed is higher than 180 rpm. Furthermore, operation with $Bo_\omega < 20$ should be avoided, as gaps between stages may be closed by the liquid curvature leading to increased pressure drop. Another important feature of the Zickzack design is that the structure can be tailored to keep the apparent *F*-factor almost constant, counteracting mass transfer performance loss with increasing packing radius. Therefore, the distance between consecutive baffles is adjusted so that the same free cross-sectional area is preserved. The corresponding posi-

tions of the baffles can be determined by Eq. (2) in which Do_i is the outer diameter of baffle i and Di_{i+1} is the inner diameter of the next baffle. Thereby a tailored packing structure can be determined for a wide range of flow rates allowing for operation under optimal conditions.

In this article, Sect. 2 describes the experimental setup and procedures. In Sect. 3, the results of the overall mass transfer measurements in an RPB are presented and analyzed, starting with conventional metal knit-mesh and foam packings (Sect. 3.1), before the newly developed ZZ packing is compared (Sect. 3.2) and analyzed in terms of mass transfer performance and pressure drop followed by a comparison with the reported results for the RZB and other packing types (Sect. 3.3). Finally, the equipment size reduction resulting from HIGEE technology is evaluated by a comparison of the results of the current experimental investigation with those of a static column under similar operating conditions and the investigated test system in Sect. 3.4. Sect. 4 provides conclusions and an outlook on future work.

2 Experiments

2.1 Experimental Setup

Fig. 2 shows the pilot-scale RPB, which was developed in close collaboration with Proceler, Warsaw, with the annular-shaped rotor and different types of conventional packing used for the experiments in this study. As shown in Fig. 2, the RPB has a vapor inlet, vapor outlet, and liquid inlet at the top and has four liquid outlets at the bottom. The simplified flow diagram of the experimental setup for distillation in the RPB at total reflux under atmospheric pressure is shown in Fig. 3. The investigated case study of ethanol dehydration is one of the most investigated chemical systems in RPBs and also one of the standard test mixtures for distillation recommended by Onken and Arlt [26]. The composition of this mixture can be evaluated based on density measurements. For these measurements, a Densito 30PX by Mettler-Toledo GmbH is used, which has a density accuracy of ±0.001 g cm^{-3}. This relates to a composition accuracy of approx. ±0.4 wt %. Deionized water (0.998 g cm^{-3} at 20 °C) and absolute ethanol (0.789 g cm^{-3} at 20 °C) from Chemsolute® was used to prepare the feed mixture. The reflux flow rate is measured with a Coriolis flowmeter from Siemens having a SITRANS FC300 sensor with MASS 6000 transmitter and a flow accuracy of 0.1 % of the rate.

The design specifications of the investigated RPB and rotor are listed in Tab. 1. Further details of the RPB and rotor specifications can be found in the article by Neumann et al. [27]. For the experimental investigation, different types of conventional packings and the newly developed ZZ packing prototype were used. The major properties of the packings are listed in Tab. 2.

For the current study, two prototype Zickzack packing structures with an inner diameter of 146 mm, outer diameter of 356 mm and a height of 8 mm have been designed,

Table 1. Design specifications of the investigated RPB and internals.

Specification	Dimension
RPB casing inner diameter [mm]	860
Rotor outer diameter [mm]	400
Packing inner diameter [mm]	146
Packing outer diameter [mm]	380
Axial height of packing [mm]	10

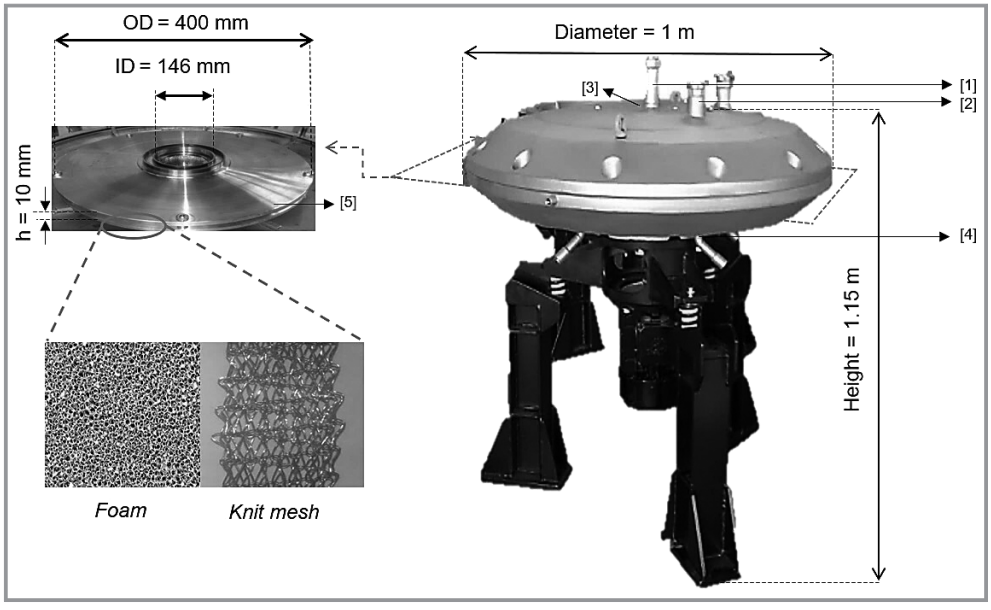

Figure 2. Pilot-scale RPB with the rotor view: 1) vapor outlet, 2) vapor inlet, 3) liquid inlet, 4) liquid outlet, 5) rotor plates.

Table 2. Properties of the investigated packings in this study.

Conventional packings	Metal knit mesh (KM)	Metal foam NCX0610	Metal foam NCX 1116	Metal foam NCX1723
Porosity ε [%]	87	92	92	92
Specific area a_p [m^2m^{-3}]	2496	500	1000	1600
Pore diameter d_p [mm]	–	2.3	1.4	0.9
Advanced packing	Zickzack 25	Zickzack 38		
Stage height h [mm]	5.5	5.5		
Protrusion lenght l [mm]	1.0	1.0		
Free cross-sectional area A_{free} [mm^2]	1888.6	1401.4		
Number of baffles [–]	25.0	38.0		
F-factor [$Pa^{0.5}$]	1.6	2.1		

which differ in the free cross-sectional area between the baffles and, thus, in the number of baffles (Tab. 2). The F-factor for the ZZ packing is calculated based on the free cross-sectional area according to Eq. (3)

$$F = \frac{\dot{m}_{v,\,out}}{\rho_{v,\,out}\, A_{free,\,i}} \sqrt{\rho_{v,\,out}} \tag{3}$$

These packing designs were produced by means of a previously developed additive manufacturing approach [24] that allows for easy and accurate manipulation of the design based on the corresponding CAD model. In contrast to the previously applied direct light processing (DLP) approach, another type of photopolymerization process was applied, using a stereolithography (SLA) approach. Here, a photosensitive liquid polymer (resin) is selectively exposed to UV laser light to form very thin solid layer upon layer (usually between 0.05–0.15 mm) to create the 3-dimensional part. The most important advantages of SLA over DLP are its bigger build size and the smooth surface of the printed object as well as a large variety of photopolymers. In this study, the packing was fabricated with a Formlabs 3D printer (Form 2), which has a build size of $150 \times 150 \times 200\ mm^3$. The layer thickness was set to 0.1 mm according to manufacturer advice and the Formlabs Hi-temp resin was selected, which has a deflection temperature up to 238 °C and moderate chemical resistance [28]. Since the build size is still not large enough to manufacture the packing in one piece, it was divided into nine pieces and bonded with Technicoll 9464 2-component epoxy adhesive, resistant to high temperatures and alcohols [29]. Fig. 4 illustrates the respective CAD model of a single packing piece with 38 baffles and the annular packing resulting from the combination of the nine single elements. To improve the mechanical stability of the packing, 72 radial rods and 186 vertical rods were added inside the structure. Further cutouts on the sides are integrated such that adjacent packing pieces position and interlock themselves during assembly of the full packing element.

2.2 Experimental Procedure

All experiments were conducted according to the same procedure. At first, the rotational speed of the RPB was fixed to

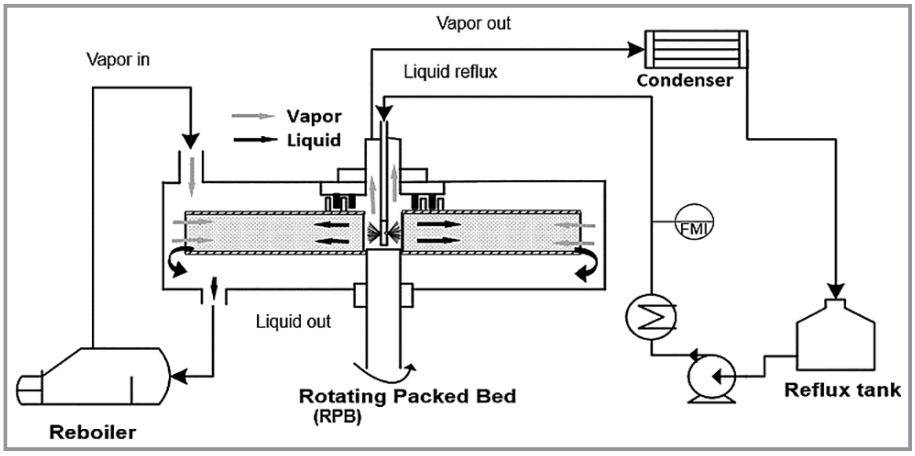

Figure 3. Flow scheme of RPB pilot plant under total reflux at atmospheric pressure.

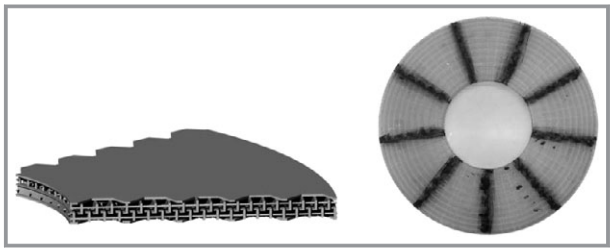

Figure 4. CAD model of Zickzack packing piece and a photo of the bonded Zickzack packing.

a value between 1–10 s^{-1} and a 10 wt % ethanol-water mixture of approximately 6 L was pumped into the reboiler via the reflux tank (Fig. 3). Nitrogen was used as an inert gas in the reboiler to ensure safe operation. It leaves the system via an inert gas outlet on the condenser. The electrically-heated reboiler was set to a power resulting in an *F*-factor of 0.6 $Pa^{0.5}$ at the eye of the rotor, defined by

$$F_{\mathrm{eye}} = \frac{\dot{m}_{\mathrm{v,\,out}}}{\rho_{\mathrm{v,\,out}}\, A_{\mathrm{c,\,i}}}\ \sqrt{\rho_{\mathrm{v,\,out}}} \tag{4}$$

where $A_{c,i}$ represents the cylindrical surface area at the inner radius of the packing, $\rho_{v,out}$ is the vapor density and $\dot{m}_{v,\,out}$ is the mass flow rate at the vapor outlet of the RPB. The vapor stream was introduced into the RPB through the vapor inlet at the outer edge of the upper casing, flows radially through the packing and leaves the RPB through the eye of the rotor. Afterward, the vapor stream was condensed in the overhead condenser and the condensate was collected in the reflux tank. A constant mass of the liquid in the reflux tank was used to control the reflux pump and to ensure operation under total reflux. A Coriolis mass flow meter was used to obtain an online measurement of the flow rate and density of the liquid reflux. Once a steady state was achieved, liquid samples were drawn from the liquid reflux and the bottom stream of the RPB. Steady state was assumed once the temperatures were steady and the density change of the liquid reflux was less than 0.0005 g cm^{-3} over 10 min. The liquid samples were further analyzed with the Mettler Toledo-Densito 30 PX. It took approximately 2 h to get the first steady state and approximately 20–30 min to achieve new steady-state operation after modifying the rotational speed. While the longer initial period for obtaining the steady state can be assigned to the heat uptake by the solid steel casing of the RPB, the short periods for reaching the new steady state indicate the capability of the RPB to quickly adjust to changes during operation. Each experimental run was performed twice. At first, the rotational speed was increased stepwise from 1 s^{-1} to 10 s^{-1}, while afterward the rotational speed was reduced stepwise in the same intervals to complete the cycle and investigate potential hysteresis effects.

To evaluate the contribution of the casing and packing to the overall mass transfer, PT100 thermocouples were installed at the vapor inlet, outlet and in the casing of the RPB. The vapor compositions were determined based on vapor-liquid equilibria calculated on the basis of the temperature measurement at 101.325 kPa [23]. The vapor pressure of the pure components was calculated using the Antoine equation, Eq. (5)

$$\log P[\mathrm{mmHg}] = A - \frac{B}{T[^{\circ}C] + C} \tag{5}$$

The relative volatility and equilibrium phase composition were calculated from Eq. (6) and Eq. (7), respectively

$$\alpha = \frac{P_1\gamma_1}{P_2\gamma_2} \tag{6}$$

$$y^{*} = \frac{\alpha\, x}{x(\alpha - 1) + 1} \tag{7}$$

The activity coefficient γ_i of each component was estimated according to the NRTL model with database APV88 VLE-IG:

$$\begin{aligned} \ln(\gamma_1) &= x_2^2\left[\tau_{21}\left(\frac{G_{21}}{x_1 + x_2}\right)^2 + \tau_{12}\frac{G_{12}}{(x_2 + x_1 G_{12})^2}\right] \\ \ln(\gamma_2) &= x_1^2\left[\tau_{12}\left(\frac{G_{12}}{x_1 + x_2}\right)^2 + \tau_{21}\frac{G_{21}}{(x_1 + x_2 G_{21})^2}\right] \end{aligned} \tag{8}$$

$$G_{\mathrm{ij}} = \exp\left(-0.3\,\tau_{\mathrm{ij}}\right), \quad \tau_{\mathrm{ij}} = \frac{A_{\mathrm{ij}}}{RT} \tag{9}$$

3 Results and Discussion

At first, the mass transfer performance of the conventional packings in RPB is evaluated and the results are compared with literature data to provide validation and extend the comparison to other advanced packings. Afterward, the newly developed ZZ packing is evaluated with respect to the conventional packings and literature performance data for the RZB. Finally, a comparison with structured packings in a static packed column is conducted to evaluate the potential of the RPB with ZZ packings for process intensification.

To analyze the mass transfer performance of the specific RPB, the number of theoretical stages (N_{th}) and the resulting *HETP* value are used as a measure of overall and packing-specific separation efficiency. This allows for better comparability of performance data with respect to the dimensions of the investigated RPB and packing, compared to the regularly derived overall volumetric mass transfer rates ($k_G a$ or $k_L a$), which are most often calculated based on the integral performance data for the whole RPB, related to the volume of the installed packing [13, 14, 16]. It furthermore is of added value for the subsequent analysis regarding the mass transfer contributions of the packing and the casing. The number of theoretical stages is calculated based

on an analytical description of the vapor-liquid equilibrium curve. Since ethanol-water is a non-ideal system, the change of relative volatilities (α) with the change of liquid composition is estimated by using the empirical approach proposed by Li et al. [30]. Details of the method are described in the Appendix.

3.1 Comparison of Conventional Packing Types: Metal Foams with Metal Knit Mesh

In Fig. 5, the overall number of theoretical stages and pressure drop of the RPB are plotted for metal knit mesh and three investigated metal foams differing mainly in the pore diameter and specific surface area.

At the specified *F*-factor a reflux liquid flow rate of approx. 10 kg h^{-1} is obtained, which corresponds to a liquid load [27] of approx. 2.6 m^{3}m^{-2}h^{-1} at the inner radius of the packing. The shape of the N_{th} curves in Fig. 5 for the three types of metal foams can be divided into two sections. To distinguish both, the optimal rotational speed (n_{opt}) is defined as the one giving the maximum number of theoretical stages at the investigated conditions. In the first section ($n \leq n_{opt}$) the separation efficiency increases with rotational speed, while in the second section ($n > n_{opt}$) an opposite relation is observed. These results clearly indicate a trade-off between contacting time or liquid holdup in the packing and effective interfacial area as previously analyzed by Qammar et al. [23]. This trade-off is further observed during the liquid holdup measurements using γ-ray tomography by Gross et al. [31], who clearly documented the decreasing liquid holdup in the packing with increasing rotational speed as well as increasing the radial depth of the packing [32].

In the conventional column, the liquid flows under the influence of gravitational acceleration (10 m s^{-2}), whereas in an RPB the liquid flows under the influence of centrifugal acceleration, which is several times higher than the gravitational acceleration. Therefore, the contact time between the vapor and the liquid in an RPB is much shorter than in a column. Although the interfacial area is increased as a result of fine droplet generation or thin films at higher rotational speeds, there exists at a certain rotational speed a trade-off between the increased interfacial area and decreased contact time marked by the optimal rotational speed. Other authors, e.g., Chu et al. [33] and Luo et al. [15] also analyzed analogous behavior for the methanol-water system in a continuous distillation two-stage countercurrent RPB (TSCC-RPB). Furthermore, it can be seen from Fig. 5 that the metal foam NCX0610, which has the largest pore diameter and the lowest specific geometrical surface area, does not only provide the lowest pressure drop but also outperforms the other metal foams in respect to the measured N_{th} values. Possible reasons for the lower N_{th} values of the metal foams NCX1116 and NCX1723, despite their higher specific geometrical surface area, maybe liquid channeling in the pores or complete filling of some pores by the liquid due to the smaller pore diameter. This might lead to a bypass of vapor through the open pores and, hence, less vapor-liquid contact in the packing. Nevertheless, all the metal foams show maximum separation efficiency at a rotational speed of ~200 rpm, which does not exceed two theoretical stages, accounting for the whole RPB.

The separation efficiency curve for the metal knit mesh has the same trend as the metal foams but providing a higher separation efficiency of almost 2.5 theoretical stages at a slightly higher rotational speed. The overall superior mass transfer performance of the knit mesh can be related to the significantly higher specific geometric surface area of ~2500 m^{2}m^{-3}, which can be directly related to the higher interfacial area between gas and liquid. It is assumed that the higher specific geometric surface area does not provide any benefit in case of metal foams due to the reason that the pore size is decreasing with increasing specific geometric surface area while keeping the porosity constant (Tab. 2). It may result in a fraction of small pores being filled with liquid and not directly contacting with the vapor phase, and thus, decreasing the mass transfer performance of the packing, whereas in a knit mesh the structure of the knit mesh or wires is more open, thus, facilitating vapor-liquid contact. However, the increase in separation performance of knit mesh comes at the cost of the higher pressure drop as depicted in Fig. 5.

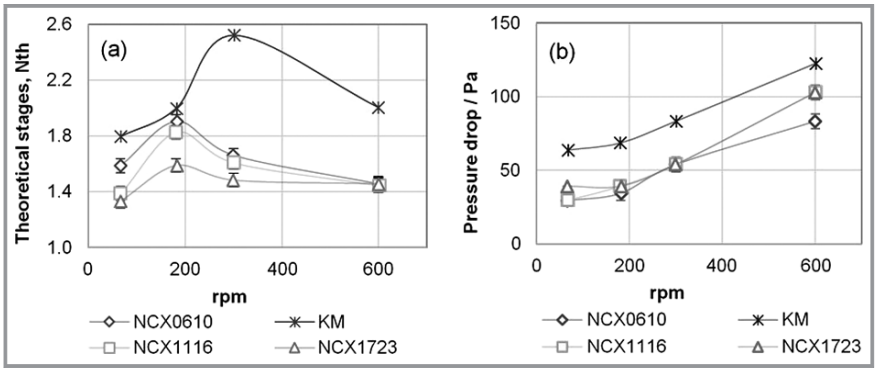

Figure 5. Effect of rotational speed on mass transfer performance (a) and pressure drop (b) of investigated metal knit mesh and metal foams for distillation in RPBs; F_{eye} = 0.6 Pa$^{0.5}$.

3.2 Comparison of the Advanced Zickzack Packing with Knit Mesh

The same experimental procedure was used for testing the performance of the ZZ packing as used for knit mesh and metal foams. Performance evaluation of both variants of ZZ packing, i.e., ZZ-25 and ZZ-38, showed that ZZ-25 provided better mass transfer performance. This can be related to the larger free cross-

sectional area of ZZ-25 for vapor-liquid contacting. A narrower annular gap in ZZ-38 leads to higher velocity and corresponding higher *F*-factor (Tab. 2). These results are in agreement with the literature results of RZB [34] and other classical packings [13] that show that increasing the *F*-factor after a certain value leads to poorer performance [34]. A comparison of the mass transfer (Fig. 6) and hydrodynamic performance (Fig. 6) of ZZ-25 packing and the knit mesh (the best available among conventional packings) is illustrated in Fig. 6. The superior mass transfer performance of the ZZ packing is associated with the higher liquid holdup and more homogeneous hydrodynamics in the packing. Below 180 rpm sudden increase in pressure drop can be noted, which is the result of the increasing liquid curvature on packing stages. Due to this fact, the gap between stages is obscured and available cross-sectional area for gas flow is decreased. Eventually, that leads to the entrainment of liquid and flooding of the packing due to a higher gas velocity.

3.2.1 Contribution of Packing and Casing to the Overall Mass Transfer

While the presented experimental results for the different packings indicate the importance of the selection of an optimal packing for an efficient separation in an RPB, the reported N_{th} values are only valid for the whole RPB and are not suited for the derivation of packing-specific *HETP* values or overall volumetric mass transfer rates ($k_G a$ or $k_L a$). For an accurate characterization of the separation performance of a specific packing and as a consequence a reliable scale-up, it is important to determine the actual contribution of the packing and the casing to the overall separation efficiency. As indicated in previous investigations [23] there can be a substantial contribution of the casing to the overall separation efficiency. The results of temperature measurements at the vapor inlet, in the casing and at the vapor outlet indicate that the casing contributes almost an equivalent to one theoretical stage to the overall mass transfer in the RPB, as illustrated in Fig. 7.

These results align with theoretical considerations derived by the correlations of Burns et al. [35] for liquid holdup and also with the liquid holdup measurements using γ-ray tomography by Gross et al. [32], which indicate that the liquid holdup in the packing decreases significantly with increasing rotational speed while the contribution of the casing to the overall mass transfer increases due to reduced mass-transfer in the packing [23]. At the previously determined maximum separation efficiency, the contribution of the casing is determined to be 0.77 and the contribution of the packing to be 1.86 theoretical stages, resulting in a fraction of only 71 % of the mass transfer happening inside the packing. Therefore, for the development of scale-up and design rules it is important to consider that not all the mass transfer happens in the packing and that depending on the dimensions of the packing, the casing, and the rotational speed, the mass transfer in the casing can be decisive compared to the mass transfer inside the packing, as it is the case for rotational speed of 900 rpm in Fig. 7.

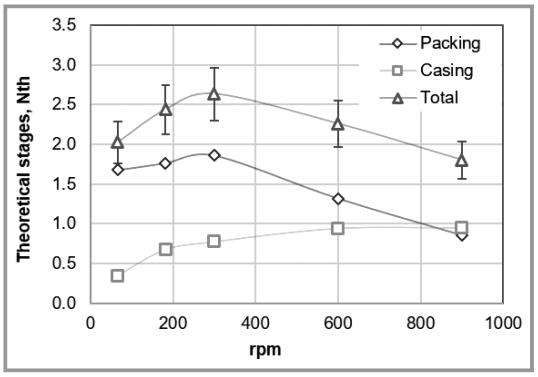

Figure 7. Mass transfer contribution of the packing and the casing to the overall mass transfer in an RPB using temperature measurements at vapor inlet, outlet and in the casing; $F_{eye} = 0.6\ Pa^{0.5}$, knit mesh packing.

In Fig. 8, the mass transfer inside the packing is further analyzed based on the temperature measurements, as described above. The figure illustrates the relative contribution of the packing to the overall mass transfer, based on the relation between the vapor compositions, $(y_{out} - y_{casing})\,(y_{out} - y_{in})^{-1}$ [23].

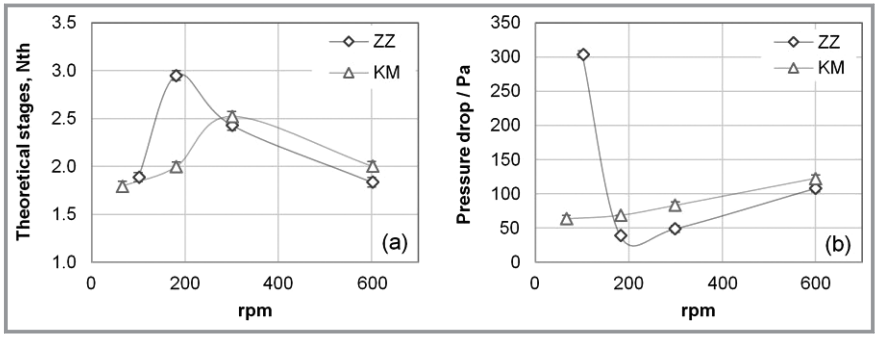

Figure 6. Mass transfer (a) and hydrodynamic (b) comparison of Zickzack (ZZ) packing with knit mesh (KM); $F_{eye} = 0.6\ Pa^{0.5}$.

3.3 Comparison with Other Packing and Rotor Designs Reported in Literature

In light of the preceding analysis of the mass transfer contributions of packing and casing to the overall mass transfer of the RPB, the experimentally determined separation performance of the conventional packing materials is further analyzed with respect to reported literature results for distillation experiments with similar systems and different

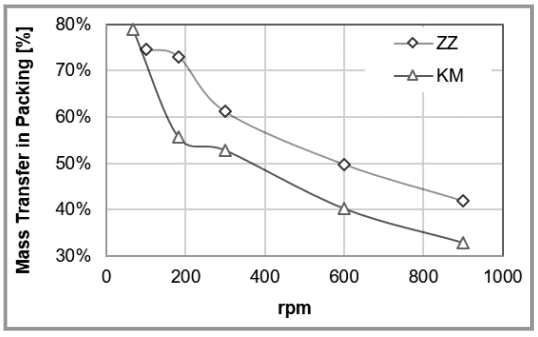

Figure 8. Comparison of packing contribution to overall mass transfer for Zickzack (ZZ) and knit mesh (KM); F_{eye} = 0.6 $Pa^{0.5}$ [23].

types of packing. Tab. 3 lists the design and operation specifications of the investigated split packing, metal foam, and RZB in the literature. From the reported data, the maximum separation efficiency at F_{eye} of 0.6 $Pa^{0.5}$ was selected as a reference for comparison, since separation efficiency is a function of rotational speed. For RZB, Wang et al. [34] investigated mass transfer and hydrodynamic performance of eleven different baffle structures for ethanol dehydration in RZB. Among these baffle design options, data at an *F*-factor of 1.6 $Pa^{0.5}$ (based on the free cross-sectional area between two baffles) is available for three of these baffle structures, i.e., R-3, R-8, and R-9. R-3 is a regular baffle structure for RZB whereas R-8 and R-9 are the advanced forms of baffle structure with few layers of metal gauze packing mounted on the baffle. For comparison, R-3 and R-9 are chosen since R-3 is the characteristic baffle design of an RZB and from the advanced baffle, design R-9 shows better mass transfer performance [34].

HETP values are determined based on the reported geometrical data for the inner and outer radius of the specific packing

$$HETP = \frac{(r_o - r_i)_{packing}}{N_{th}} \quad (10)$$

Furthermore, besides the *HETP* value that is based on the reported separation efficiency for the respective RPB, a refined *HETP* value is determined that considers a maximum casing contribution equivalent to one theoretical stage for the reported mass transfer results and is calculated according to Eq. (11)

$$HETP_{refined} = \frac{(r_o - r_i)_{packing}}{N_{th} - 1} \quad (11)$$

The comparison of the *HETP* values resulting from the current study (based on N_{th} in Fig. 5 and Fig. 6) and the literature data (Tab. 3) is illustrated in Fig. 9. The comparison of the experimental results of the current study and the literature data on the metal foam agree very well. While the knit mesh outperforms the metal foam further improvement potential can be realized through the more complex rotor modifications in an RZB (one static and one rotating disc) and the split packing (two oppositely rotating discs). However, to the best of our knowledge, no industrial application has been reported so far for the split packing. On the contrary, several hundred industrial applications of RZB in continuous distillation in China have been reported [2, 7]. Besides the improved separation performance in distillation, compared to wire mesh and metal foams, additional benefits, such as the potential for an intermediate feed and the possibility to operate without specific liquid distributors further foster the applicability of RZB [18]. However, due to the increased friction through the static and rotating baffles on the opposing discs a higher pressure drop and power consumption result for the RZB compared to single-block packings in RPB, which provides further potential for improvement [18].

As can be seen from Fig. 9, excluding the contribution of the casing, an *HETP* value of 5.3 cm is found for the ZZ packing at the maximum separation efficiency, which is comparable to the two variants of RZB. However, an RZB offers a pressure drop of approx. 138–158 Pa per theoretical stage at an *F*-factor of 1.6 $Pa^{0.5}$ depending upon the baffle design used [34], as compared to a pressure drop of approx. 14 Pa per theoretical stage, for the ZZ packing. Thus, the initial experimental results for the ZZ packing indicate that a comparable separation efficiency to RZB can be obtained at a significantly reduced pressure drop. Moreover, the electrical power consumption as measured for an RPB at the rotational speed that gives the maximum separation efficiencies, i.e., 181 rpm for ZZ and 300 rpm for KM, is 83 W and 138 W, respectively. Whereas the power consumption

Table 3. Design and operation specifications of the compared packing (split packing, metal foam) and rotor types (RZB).

	Reference	Packing specifications	Test system conditions	F_{eye} [$Pa^{0.5}$]	*HETP* [m]
a)	Mondal et al. [14] (split packing)	d_i = 0.6 m, d_o = 0.31 m, h = 0.027 m, a_p = 280 m^2m^{-3}	methanol-ethanol, total reflux, 101.325 kPa	0.36–0.6	0.029–0.15
b)	Wang et al. [34], (RZB)	d_i = 0.11 m, d_o = 0.28 m, h = 0.06 m, rotor R-3, R-9	ethanol-water, total reflux, 101.325 kPa	0.4–3.6	0.021–0.042
c)	Kelleher and Fair [13] (metal foam or sponge)	d_i = 0.175 m, d_o = 0.6 m, h = 0.15 m, a_p = 2500 m^2m^{-3}	cyclohexane-*n*-heptane, total reflux, 165.5 kPa	0.6–1.2	0.038–0.072

Note: Values are estimated from the reported literature data [13, 14, 34].

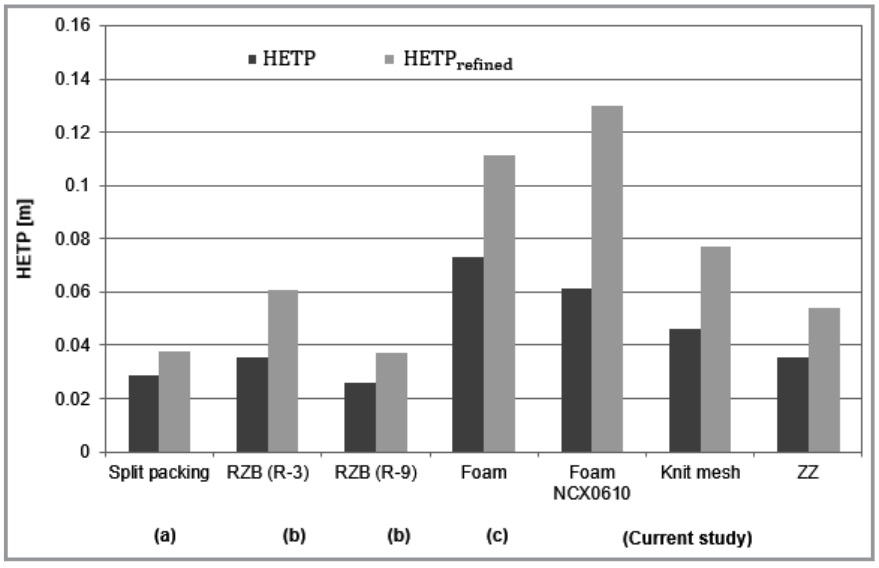

Figure 9. Refinement and comparison of literature results a), b), and c) [13, 14, 34] for the different rotor and packing types with results of the current study (ZZ, foam NCX0610 and knit mesh).

for the two variants of RZB (R-3 and R-9), as estimated from the published data is approx. 250 W [30, 34].

3.4 Comparison with Static Column

In order to compare the resulting *HETP* values with static column data, a random packing, Raschig super ring metal (RSRM) and an industrially used structured packing, HOLPACK, taken from Darakchiev and Semkov are considered [36]. The experimental data originates from the binary distillation of ethanol-water mixture under total reflux conditions in a column with an inner diameter of 0.213 m and a packing height of 2.8 m [36]. As can be seen from Fig. 10, a reduction of the *HETP* value of 4–10-fold can be achieved with an RPB under the investigated operating conditions. Moreover, the packing volume required in the RPB or RZB would be much less than that of the column [18, 19], which opens the possibility of using specialized

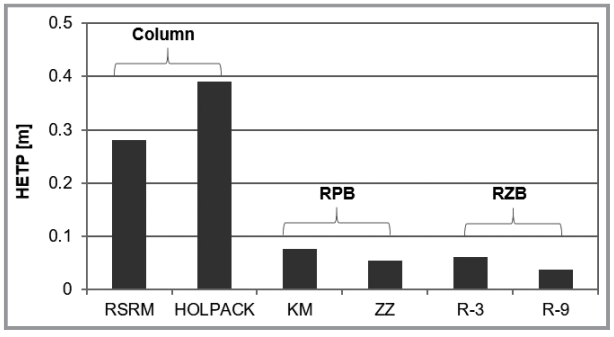

Figure 10. Comparison of *HETP* values of static column with different packing and rotor types in an RPB; *F*-factor = 0.6 $Pa^{0.5}$ for RSRM, HOLPACK and KM; *F*-factor = 1.6 $Pa^{0.5}$ for ZZ, R-3 and R-9.

packing for certain processes despite the high cost of this specific packing. Considering the initially proposed potential for process intensification, quantified by Ramshaw and Mallinson [21] as a reduction of 10–100-fold in *HETP*, it has to be concluded that the current and literature results are rather close to the lower end of this ambitious range [11, 13, 14, 34]. With the conventional metal foam and knit mesh packings, a reduction of approx. 2 – 5-fold in *HETP* can be achieved compared to conventional packed columns [11, 36], while the results for the split packing, RZB, and ZZ packing indicate the possibility for a 7–10-fold reduction.

4 Conclusions

In this article, the results of a systematic experimental approach for the development of packing design for distillation operation in RPBs are presented comparing the properties, hydrodynamic and mass transfer performance of different conventional packings in a single-rotor RPB under total reflux distillation experiments. The detailed analysis of the mass transfer contributions in the packing and casing show an important need to clearly differentiate these contributions for reliable quantification of the performance of the whole RPB. It was found that the separation efficiency of the knit mesh is the highest among the investigated conventional packing types though at the cost of higher pressure drop, while other improved designs like split packing and RZB allow for further improvements in terms of the mass transfer. The newly developed Zickzack packing provides comparable separation efficiency to RZB with about 10 times lower pressure drop and bears the potential for a reduction of approx. 8-fold in the *HETP* value compared to conventional static packed columns. Yet, there is a lot of potential to optimize the design of the Zickzack packing, through modification of the height of the packing, the baffles, the weir and also their geometrical form. These investigations will be performed in further research, which will also evaluate the mass transfer performance with larger radial depth and larger vapor and liquid flow rates, which is important to provide reliable data for process design.

The research leading to these results was done in cooperation with the Institute of Sustainable Process Technology (ISPT) in the frame of the project ImPaCCt (Improved Process Performance by Process Intensification in Centrifugal Contactors). H.Q. would also like to gratefully acknowledge the scholarship by Higher Education Commission (HEC), Pakistan, in cooperation with Deutscher Akademischer Austauschdienst (DAAD) under the funding program, faculty development of M.Sc. leading to Ph.D. for UESTP Germany. Furthermore, M.S. gratefully acknowledges financial support from the Max-Buchner Research Foundation.

Appendix

The number of theoretical stages (N_{th}) is calculated by using an analytic description of the vapor-liquid-equilibrium (VLE) curve. The general VLE curve of a binary and ideal system can be defined by Eq. (A1). In the case of a non-ideal system, the relative volatilities (α) change with the liquid composition. In this regard, Li et al. [30] proposed an empirical approach, Eq. (A2), where they correlated the relative volatility of the ethanol-water system (α) with the liquid composition (x_E) by a composite function and five empirical constants (a – e).

$$y^{\star} = \frac{\alpha\, x}{x(\alpha - 1) + 1} \tag{A1}$$

The Excel® solver was utilized to minimize the *RMS* of the absolute error between the property data obtained from Aspen Plus® V8.8 (NRTL property method with database APV88 VLE-IG) and the VLE data calculated with equation

$$\alpha = \begin{cases} a(x_E + b)^c & x_E \le 0.292 \\ d(x_E)^e & x_E > 0.292 \end{cases} \tag{A2}$$

The empirical constants from Li et al. [30] served as starting values. The final best-fit constants, together with the calculated *RMS*, are listed in Tab. A1. With the explicit description of the VLE curve, the number of theoretical stages (N_{th}) can be calculated together by employing total reflux criteria ($x = y$) in an iterative fashion.

Table A1. Regression constants for the analytic description of the relative volatilities of the ethanol-water system.

	Li et al. [30]	Current work
a	1.1213	1.1213
b	0.2	0.194
c	–1.523	–1.524
d	0.8938	0.9136
e	–1.062	–1.062
RMS [%]	0.56	0.29

Symbols used

$A_{c,I}$	[m^2]	flow area at the eye of the rotor
$A_{free,I}$	[mm^2]	free cross-sectional area between two consecutive baffles
a_p	[m^2m^{-3}]	specific surface area
Bo	[–]	Boden number
d_i	[mm]	inner diameter of rotor
d_o	[mm]	outer diameter of the rotor
d_p	[mm]	pore diameter
F_{eye}	[$Pa^{0.5}$]	*F*-factor at the eye of the rotor
h	[mm]	packing height
HETP	[m]	height equivalent to a theoretical plate
$\dot{m}_{v,out}$	[kg s^{-1}]	mass flow rate of vapor
n	[rpm]	rotational speed
n_{opt}	[rpm]	optimal rotational speed
N_{th}	[–]	number of theoretical stages
P	[mmHg]	saturated vapor pressure of pure component
T	[°C]	temperature
x	[mol mol^{-1}]	mole fraction of ethanol in the liquid phase
y	[mol mol^{-1}]	mole fraction of ethanol in the vapor phase
$y^{\star}$	[mol mol^{-1}]	equilibrium mole fraction of ethanol in the vapor phase

Greek letters

α	[–]	coefficient of relative volatility
ε	[–]	porosity
γ_1	[–]	activity coefficients of ethanol
γ_2	[–]	activity coefficients of water

Abbreviations

HIGEE	high gravity
KM	knit mesh
ID	inner diameter
OD	outer diameter
RPB	rotating packed bed
RSRM	Raschig super ring metal
RZB	rotating zigzag bed
ZZ	Zickzack packing

References

[1] *Distillation: Fundamentals and Principles* (Eds: A. Gorak, E. Sorensen), 1st ed., Academic Press, San Diego **2014**.

[2] G. Q. Wang, Z. C. Xu, J. B. Ji, *Chem. Eng. Res. Des.* **2011**, *89 (8)*, 1434–1442. DOI: https://doi.org/10.1016/j.cherd.2011.02.013

[3] G. E. Cortes Garcia, J. van der Schaaf, A. A. Kiss, *J. Chem. Technol. Biotechnol.* **2017**, *92 (6)*, 1136–1156. DOI: https://doi.org/10.1002/jctb.5206

[4] D. P. Rao, A. Bhowal, P. S. Goswami, *Ind. Eng. Chem. Res.* **2004**, *43 (4)*, 1150–1162. DOI: https://doi.org/10.1021/ie030630k

[5] L. Agarwal, V. Pavani, D. P. Rao, N. Kaistha, *Ind. Eng. Chem. Res.* **2010**, *49 (20)*, 10046–10058. DOI: https://doi.org/10.1021/ie101195k

[6] D. P. Rao, *Indian Chem. Eng.* **2015**, *57 (3–4)*, 282–299. DOI: https://doi.org/10.1080/00194506.2015.1026946

[7] K. Neumann, K. Gladyszewski, K. Groß, H. Qammar, D. Wenzel, A. Górak, M. Skiborowski, *Chem. Eng. Res. Des.* **2018**, *134*, 443–462. DOI: https://doi.org/10.1016/j.cherd.2018.04.024

[8] W. J. Podbielniak, *US2004011*, **1935**.

[9] P. C. Wilhelm, D. S. Wilhelm, *US2941872A*, **1960**.

[10] C. Ramshaw, R. H. Mallinson, *US 4283255*, **1981**.

[11] C. C. Lin, T. J. Ho, W. T. Liu, *J. Chem. Eng. Jpn.* **2002**, *35 (12)*, 1298–1304. DOI: https://doi.org/10.1252/jcej.35.1298

[12] K. Neumann, S. Hunold, M. de Beer, M. Skiborowski, A. Górak, *Ind. Eng. Chem. Res.* **2018**, *57 (6)*, 2258–2266. DOI: https://doi.org/10.1021/acs.iecr.7b04186

[13] T. Kelleher, J. R. Fair, *Ind. Eng. Chem. Res.* **1996**, *35 (12)*, 4646–4655. DOI: https://doi.org/10.1021/ie950662a

[14] A. Mondal, A. Pramanik, A. Bhowal, S. Datta, *Chem. Eng. Res. Des.* **2012**, *90 (4)*, 453–457. DOI: https://doi.org/10.1016/j.cherd.2011.08.008

[15] Y. Luo, G. Chu, L. Sang, H. Zou, Y. Xiang, J. Chen, *Chin. J. Chem. Eng.* **2016**, *24 (1)*, 109–115. DOI: https://doi.org/10.1016/j.cjche.2015.06.015

[16] C.-C. Lin, Y.-C. Lin, K.-S. Chien, *J. Ind. Eng. Chem.* **2009**, *15 (6)*, 813–818. DOI: https://doi.org/10.1016/j.jiec.2009.09.005

[17] X. P. Li, Y. Z. Liu, *Chin. J. Chem. Eng.* **2010**, *18 (1)*, 55–60.

[18] G. Q. Wang, O. G. Xu, Z. C. Xu, J. B. Ji, *Ind. Eng. Chem. Res.* **2008**, *47 (22)*, 8840–8846. DOI: https://doi.org/10.1021/ie801020u.

[19] G. Q. Wang, Z. C. Xu, Y. L. Yu, J. B. Ji, *Chem. Eng. Process.* **2008**, *47 (12)*, 2131–2139. DOI: https://doi.org/10.1016/j.cep.2007.11.001

[20] G. Q. Wang, Z. C. Xu, J. B. Ji, *Chem. Eng. Res. Des.* **2011**, *89*, 1434–1442.

[21] C. Ramshaw, *Chem. Eng. (London)* **1983**, *389*, 13–14.

[22] D. Eimer, *Gas Treating: Absorption Theory and Practice*, John Wiley & Sons, Chichester **2014**.

[23] H. Qammar, F. Hecht, M. Skiborowski, A. Górak, *Chem. Eng. Trans.* **2018**, *69*, 655–660. DOI: https://doi.org/10.3303/CET1869110

[24] K. Gladyszewski, M. Skiborowski, *Chem. Eng. Process.* **2018**, *127*, 1–9. DOI: https://doi.org/10.1016/j.cep.2018.02.024

[25] V. A. Lubarda, *Acta Mech* **2013**, *224 (7)*, 1365–1382. DOI: https://doi.org/10.1007/s00707-013-0813-6

[26] U. Onken, W. Arlt, *Recommended test mixtures for distillation columns*, 2nd ed., The Institution of Chemical Engineers, Warwickshire **1990**.

[27] K. Neumann, S. Hunold, M. Skiborowski, A. Górak, *Ind. Eng. Chem. Res.* **2017**, *56 (43)*, 12395–12405. DOI: https://doi.org/10.1021/acs.iecr.7b03203

[28] www.formlabs.com/media/upload/HighTemp-DataSheet.pdf (accessed April 02, 2019)

[29] Technical Data Sheet, technicoll® 9464, Ruderer Klebetechnik GmbH, Zorneding **2016**. www.technicoll.eu/fileadmin/media/Documents/Produktinformationen_englisch/PI_technicoll_9464__GB_.pdf (accessed April 02, 2019)

[30] Y. Li, X. Li, Y. Wang, Y. Chen, J. Ji, Y. Yu, Z. Xu, *Ind. Eng. Chem. Res.* **2014**, *53 (12)*, 4821–4837. DOI: https://doi.org/10.1021/ie4019337

[31] K. Groß, A. Bieberle, K. Gladyszewski, M. Schubert, U. Hampel, M. Skiborowski, A. Górak, *Chem. Ing. Tech.* **2019**, *91 (7)*, 1032–1040. DOI: https://doi.org/10.1002/cite.201800085

[32] K. Groß, A. Bieberle, K. Gladyszewski, M. Schubert, M. Skiborowski, U. Hampel, A. Górak, in *Proc. of 9th World Congress on Industrial Process Tomography*, International Society for Industrial Process Tomography, **2018**, 831–838.

[33] G.-W. Chu, X. Gao, Y. Luo, H.-K. Zou, L. Shao, J.-F. Chen, *Sep. Purif. Technol.* **2013**, *102*, 62–66. DOI: https://doi.org/10.1016/j.seppur.2012.09.029

[34] G. Q. Wang, Z. J. Zhou, Y. M. Li, J. B. Ji, *Chem. Eng. Process.* **2019**, *135*, 141–147. DOI: https://doi.org/10.1016/j.cep.2018.11.014

[35] J. R. Burns, J. N. Jamil, C. Ramshaw, *Chem. Eng. Sci.* **2000**, *55 (13)*, 2401–2415. DOI: https://doi.org/10.1016/S0009-2509(99)00520-5

[36] S. Darakchiev, K. Semkov, *Chem. Eng. Technol.* **2008**, *31 (7)*, 1039–1045. DOI: https://doi.org/10.1002/ceat.200800029

